LIP-STUDENTS-21-00

Projected sensitivity of the LUX-ZEPLIN experiment to the $0\nu\beta\beta$ decay of ^{136}Xe

Carlos Roxo[1,a] and Francisco Pais[1,b]

[1] *Universidade de Coimbra, Coimbra, Portugal*
[2] *Instituto Superior Técnico, Lisboa, Portugal*

Project supervisor: Paulo Brás and Alexandre Lindote

December 19, 2022

Abstract. In this article we describe the optimization process and results for the sensitivity of the LUX-ZEPLIN detector to the neutrinoless double beta decay mode of ^{136}Xe. The volume parameters we calculated result in a target xenon mass of 900kg, which contains about 80 kg of ^{136}Xe. The best result for the sensitivity to this decay, calculated using a simple cut-and-count analysis, was 7.2×10^{25} years for an exposure of 1000 days. Comparatively, the latest projected sensitivity of LZ to this decay is 1.06×10^{26} years for the same exposure. The dependence of the sensitivity on energy resolution and multiple scatter rejection capability was also studied.

1 Introduction

1.1 Neutrinoless Double Beta Decay

Two neutrino double beta ($2\nu\beta\beta$) decay is a process wherein a nucleus emits two electrons and two electron antineutrinos [1, 2]. If neutrinos are Majorana fermions, a neutrinoless mode is possible ($0\nu\beta\beta$) [1, 2].

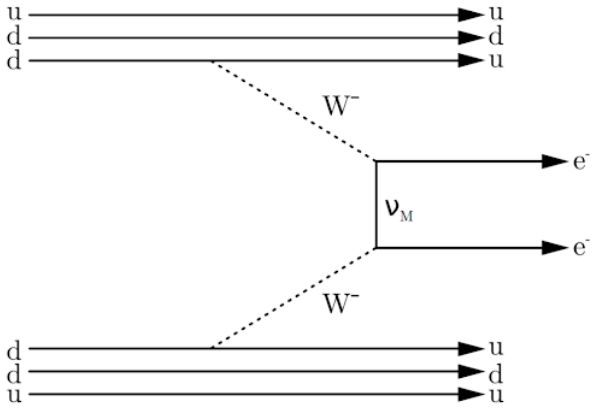

Figure 1: Feynman diagram of the neutrinoless double beta decay process mediated by the exchange of a light Majorana neutrino. [1]

Detecting $0\nu\beta\beta$ would mean the neutrino is it's own antiparticle; this would lead to a violation of lepton number invariance and perhaps pose an explanation of the matter-antimatter asymmetry observed in the universe. So far, $0\nu\beta\beta$ has not been detected.

In $0\nu\beta\beta$ all the energy in the process ($Q\beta\beta$) is taken by the electrons, meaning that a detector would only observe a monoenergetic peak in the observed energy spectrum. This is unlike what happens in $2\nu\beta\beta$ decay, in which the energy is distributed between the electrons and the neutrinos, resulting in a continuous spectrum. The experimental signature of these two decay modes is schematically represented in Figure 2.

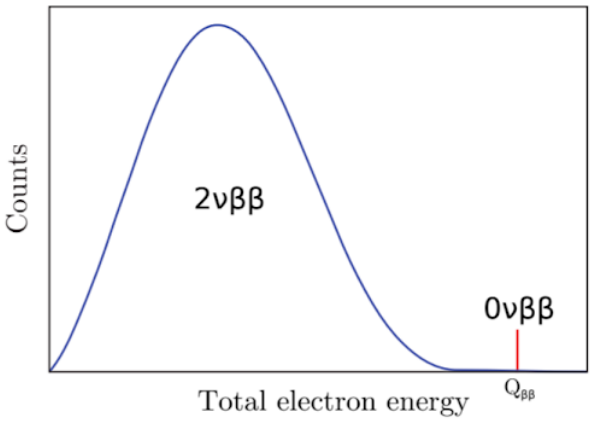

Figure 2: Schematic representation of the spectra for the two-neutrino (blue) and neutrinoless (red) double beta decay modes. [1]

If we detect an excess of background events (B) in a region of interest (ROI) around $Q\beta\beta$, it is possible to relate the $0\nu\beta\beta$ half-life sensitivity of the experiment with observed background event using:

$$T^{0\nu}_{\frac{1}{2}} = \ln 2 \frac{\varepsilon f_{ROI} \alpha N_A}{1.64 M_{Xe}} \frac{\sqrt{Mt}}{\sqrt{B\Delta E}} \quad (1)$$

where $T^{0\nu}_{\frac{1}{2}}$ is the half-life sensitivity, ε the fraction of signal that survives the cuts, f_{ROI} the fraction of signal inside the ROI, α the ^{136}Xe abundance, N_A the Avogadro's constant, M_{Xe} the molar mass of 136Xe, M the xenon mass (in the selected volume), t the exposure time (taken to be 1000 days) and ΔE the ROI's energy interval (in keV).

1.2 The LZ Detector [3]

The LZ detector is a 7 tonne dual-phase xenon time projection chamber (TPC) surrounded by an

[a] e-mail: carlosroxo7hi@gmail.com
[b] e-mail: franciscopais@tecnico.ulisboa.pt

instrumented layer of liquid xenon, dubbed "Skin", and a Gadolinium-loaded liquid scintillator detector, dubbed "outer detector". The skin and outer detector are used to veto (exclude) events with interactions in coincidence with energy depositions in the TPC. These events with interactions in more than one detector cannot be signal events, since these are expected to produce highly localized interactions in the xenon.

Photomultiplier tubes (PMTs) are distributed throughout the detector: 494 inside the main Xe chamber, 131 in the skin and 120 in the scintillator.

As LZ has a very large Xe mass, it manages to have a large mass of the relevant isotope for this study (^{136}Xe), of the same order of magnitude as the current dedicated $0\nu\beta\beta$ experiments using Xe [4, 5].

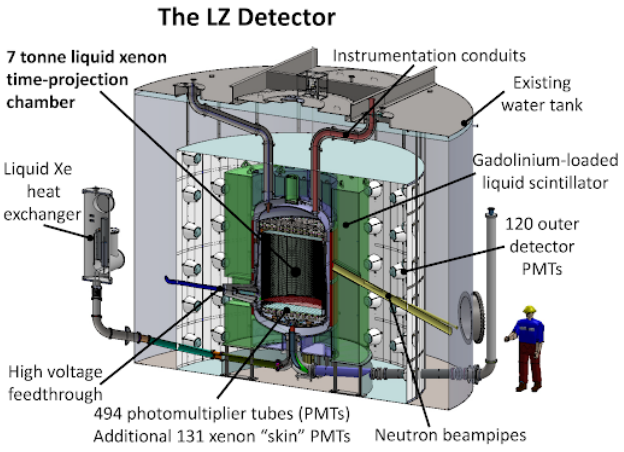

Figure 3: Schematic of the LZ Detector [6]

A particle that interacts in the active xenon volume of the TPC produces scintillation and ionization. The scintillation produces the S1 signal, while the electrons that do not recombine with the ionized atoms are drifted by an electric field onto the liquid surface and extracted to the gas, generating the S2 signal.

The time difference between the S1 and S2 signal indicates the depth of the interaction, while the light pattern of the S2 signal in the top PMT array indicates the XY position of the initial ionization site, resulting in a 3D position reconstruction of the interaction. The S1 and S2 signals are combined to obtain the energy that was deposited in the interaction.

2 Sensitivity analysis

The data used in this analysis is taken from a simulated run of LZ [3] corresponding to 1000 days of data taking. It includes most backgrounds for the neutrinoless sensitivity analysis:

- Radioactivity from detector materials (U-238 and Th-232 contaminants)
- Internal contaminants in the liquid xenon (Rn222 and daughters)
- γ-rays emitted from the cavern rocks (which also contain the contaminants mentioned above)

The objective of this work was to optimize and characterize the detector's sensitivity to $0\nu\beta\beta$ decay, by varying a set of parameters:

- Detection Volume (exclude outermost region with higher background rate)
- Energy Resolution
- Single Scatter Cut and Efficiency (rejection of events that interact multiple times with the detector)

2.1 Fiducial Volume optimization

In order to optimize the sensitivity with respect to the volume parameters, we performed two iterations of optimization. In the first, we study a large range of the volume parameters and obtained the sensitivity curve in Figure 5 for different values of the radius R, and the surface plot in Figure 6 for different values of the depth parameters Zmin and Zmax). Taking the optimal parameters from the results of the first iteration, we reiterate, now performing a finer variation over smaller ranges of R and Z, as shown in Figures 7 and 8, respectively. At last, we collect the volume parameter values for which the sensitivity is maximized, corresponding to the values R_{max}= 42cm, Z_{min}= 36cm, Z_{max}= 92cm and a sensitivity of approximately 1.9x10^{25} years.

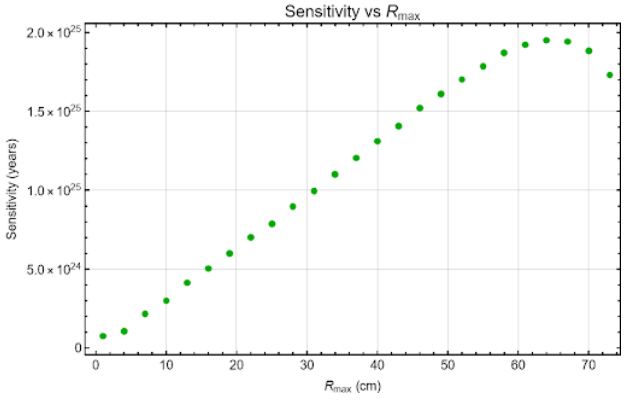

Figure 4: First variation of R_{max} with all other parameters fixed.

2.2 Energy Resolution and Single Scatter Cut

Although the energy resolution and the ability to separate multiple scatters will only be known when the detector starts operating, we can study how the sensitivity to the decay depends on these parameters. LZ is expected to reach a 1% energy resolution and a 0.3 cm single scatter rejection in the vertical direction

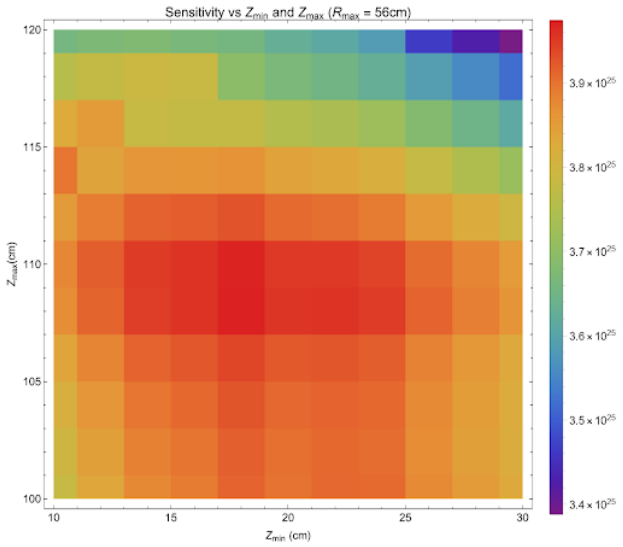

Figure 5: First variation of Z_{min} and Z_{max}.

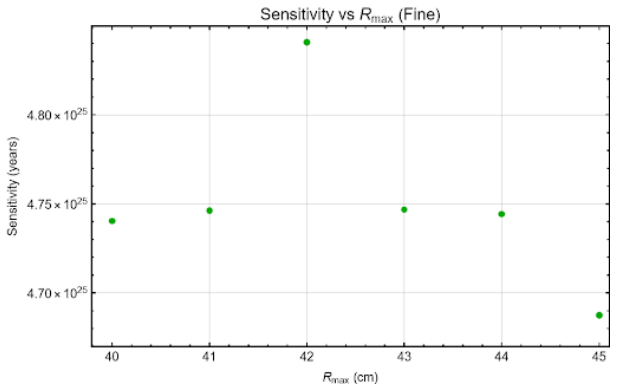

Figure 6: Second iteration of values of R_{max} for the best values of Zmin and Zmax obtained in the first iteration shown in Figure 5 (Zmin ≈ 18cm, Zmax ≈ 110).

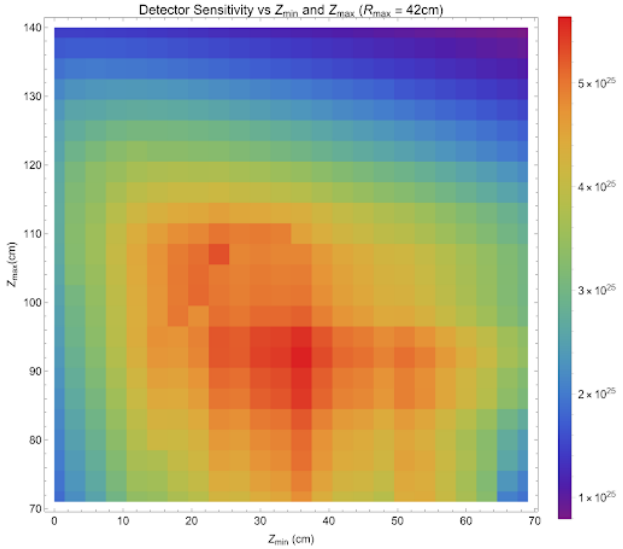

Figure 7: Second variation of Z_{min} and Z_{max} for R_{max} = 42cm, the optimized version taken from figure 6.

(these were the values used during the volume optimization performed in Section 2.1). Figure 10 shows the dependency of the sensitivity with the minimal vertical vertex separation for selecting single scatters (SS_{cut}). The best sensitivity is obtained for a 0.2 cm SS_{cut}. The decrease seen for $SS_{cut} < 0.2$ cm is due to the fact that the loss of signal events becomes greater than the loss of background when the cut becomes too small. The impact of energy resolution on sensitivity is more severe than that of SS_{cut}, as can be seen in Figure 9.

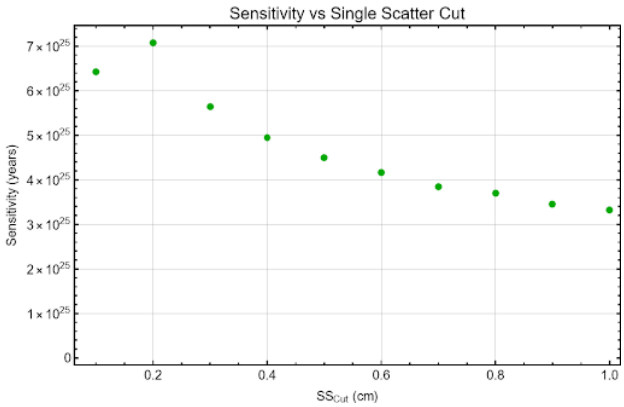

Figure 8: Sensitivity versus Single Scatter Cut, for the optimized parameters calculated in section 2.1. Note that the value used in the previous calculations was 0.3 cm.

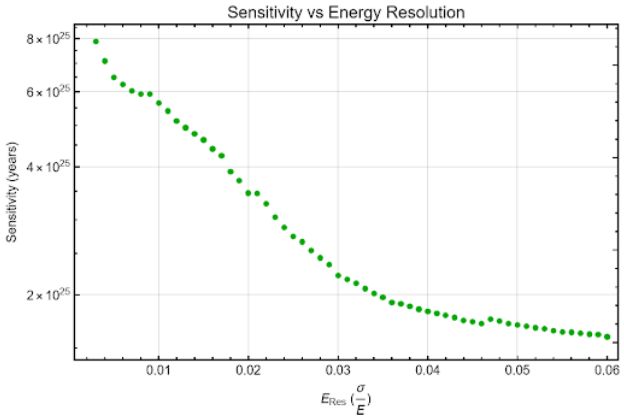

Figure 9: Sensitivity versus Energy Resolution for the optimized parameters calculated in section 2.1. Note that the energy resolution was set to 1% for all other calculations.

3 Conclusion

For an energy resolution of 1%, we estimate a maximum sensitivity of 7.2 × 10^{25} years obtained using the parameter values R_{max}= 42cm, Z_{min}= 36cm, Z_{max}= 92cm and SS_{cut}= 0.2cm. For comparison, the projected sensitivity determined by the LZ collaboration using a more sophisticated Profile Likelihood Ratio statistical analysis is 1.06 ×10^{26} years for 1000 live days of the experiment [7], at 90% confidence level) In

addition, the Xe mass in the fiducial volume is M_{Xe} = 899 kg. For an abundance of 8.9%, that corresponds to $M_{^{136}Xe}$=80kg.
^{136}Xe is currently the most sensitive isotope used to measure the Majorana mass and, therefore, provides the strongest constraints to the effective Majorana neutrino mass and is currently the best probe to the neutrino mass hierarchy. Figure 10 shows the sensitivity of LZ to the effective Majorana neutrino mass ($m\beta\beta$) obtained in this work and compared to the official projection from the LZ collaboration.

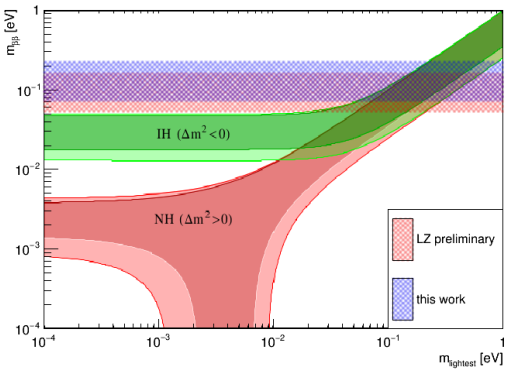

Figure 10: Final results for the sensitivity of LZ to the Majorana mass. The LZ preliminary and the results presented in this work overlap in a large region.

The expected LZ results are as good as the current best result from dedicated experiments (KamLAND-Zen) [8]. These results show that LZ can search for these rare decays despite being primarily designed for dark matter searches. It also demonstrates that dual-phase xenon TPCs are excellent multi-purpose rare event search detectors, being sensitive to a wide range of rare processes and new physics.

References

[1] S. Dell'Oro, S. Marcocci, M. Viel, F. Vissani, Advances in High Energy Physics **2016** (2016)
[2] M.J. Dolinski, A.W.P. Poon, W. Rodejohann, Ann. Rev. Nucl. Part. Sci. **69**, 219 (2019), 1902.04097
[3] D.S. Akerib et al. (LZ), Nucl. Instrum. Meth. A **953**, 163047 (2020), 1910.09124
[4] A. Gando, Y. Gando, H. Hanakago, H. Ikeda, K. Inoue, R. Kato, M. Koga, S. Matsuda, T. Mitsui, T. Nakada et al., Physical Review C **85** (2012)
[5] J.B. Albert et al. (EXO-200), Nature **510**, 229 (2014), 1402.6956
[6] D.S. Akerib, C.W. Akerlof, A. Alqahtani, S.K. Alsum, T.J. Anderson, N. Angelides, H.M. Araújo, J.E. Armstrong, M. Arthurs, X. Bai et al., Physical Review C **102** (2020)
[7] D.S. Akerib, C.W. Akerlof, A. Alqahtani, S.K. Alsum, T.J. Anderson, N. Angelides, H.M. Araújo, J.E. Armstrong, M. Arthurs, X. Bai et al., Physical Review C **102** (2020)
[8] A. Gando et al. (KamLAND-Zen), Phys. Rev. Lett. **117**, 082503 (2016), [Addendum: Phys.Rev.Lett. 117, 109903 (2016)], 1605.02889